Proceedings of the 6th International Conference on Fluid Flow and Thermal Science (ICFFTS 2025)
Barcelona, Spain - October 29 - 31, 2025
Paper No. 140
DOI: 10.11159/icffts25.140

Numerical Investigation of Self-Sustained Fluctuations in a Supersonic Impinging Jet

Muhammad Bilal*, Igor Klioutchnikov, Karl Alexander Heufer
Chair of High-Pressure Gas Dynamics, RWTH Aachen University
Schurzelter Str. 35, 52074 Aachen, Germany
*The Sirindhorn International Thai-German Graduate School of Engineering
1518 Pracharat 1 Road, Wongsawang Bangsue, Bangkok 10800, Thailand
bilal@hgd.rwth-aachen.de; klioutchnikov@hgd.rwth-aachen.de; heufer@hgd.rwth-aachen.de

Abstract **-** Coherent low-frequency pulsations produced by supersonic impinging jets impose severe acoustic and thermal loads. Yet a clear criterion for predicting the onset of discrete tones remains elusive. This study performs high-order numerical simulations of a circular jet impinging on a flat plate to isolate the governing parameters. Three controls are explored separately: nozzle pressure ratio (NPR), convective Mach number (Mc=0.82–1.20), and nozzle-to-plate spacing (h=30, 40, 50 mm). The flow is solved with a fifth-order WENO scheme using in-house solver KICK (Kinetics Computational Kernel). A centrally positioned pressure probe, located just above the nozzle exit, records the unsteady signal; Fourier analysis then extracts the dominant frequency and its corresponding Strouhal number. Results show that changing exit pressure alone leaves the pulsation essentially unchanged, whereas raising the convective Mach number (Mc) toward unity sharply suppresses the feedback loop. For Mc>1 the spectrum becomes broadband, and Strouhal numbers fall below 0.30; for Mc<1, a strong single tone persists within the canonical 0.30 – 0.70 window. Varying plate spacing mainly shifts amplitude while leaving the dominant frequency essentially unchanged. The study therefore provides a concise, design-oriented guideline: the onset of periodic fluctuations in impinging jets is dictated primarily by the convective Mach number rather than static pressure, offering a clear control parameter for launch-pad noise reduction and Vertical Take-off and Landing (VTOL) exhaust design.

Keywords**:** supersonic impinging jet, acoustic feedback loop, convective Mach number, Strouhal number

1. Introduction

Predicting and controlling the extreme unsteadiness of supersonic jets impinging on nearby structures remains a limiting issue for reusable launch vehicles, retropropulsive landing, VTOL operations, and high-speed thermal surface processing [1]. Intermittent low-frequency pressure loads, intense localized heat flux, and discrete acoustic tones all stem from self-sustained flow acoustic feedback mechanism whose onset and suppression remain hard to predict. An agreed physics-based criterion identifying which parameter (e.g., plate spacing (h), nozzle pressure ratio (NPR), or convective Mach number (Mc)) governs onset or suppression is still absent, complicating design and mitigation.

When an under-expanded jet leaves a converging–diverging nozzle and strikes a nearby flat plate, a repeating shock (diamond) pattern forms, and a Mach disk slows the jet core. The flow then turns and spreads radially as a wall jet, creating a toroidal recirculation bubble between the incoming core and the outward flow. Around this bubble, a shear layer develops and, under some conditions, a self-sustained flow–acoustic feedback loop appears. Jet impingements generate wave that travel back toward the nozzle and are associated with the next cycle of large-scale unsteadiness. Under other operating conditions, this organized loop does not establish, and the jet remains comparatively steady [2].

Extensive experiments using schlieren imaging, PIV, and microphone or hot-wire probes have mapped how nozzle-pressure ratio, plate spacing *h,* and geometry affect whether an impinging jet emits an acoustic feedback and how strong it is. Reported "onset" thresholds still disagree, and no single non-dimensional predictor is accepted. Two candidates appear most often. Mc is the ratio of the relative jet-to-ambient velocity to the sum of their sound speeds; it gauges how readily pressure waves can travel upstream through the mixing layer. The Strouhal number *St* is a non-dimensional frequency obtained with the jet speed and plate gap; reported tones almost always fall in the narrow band $0.3 \leq St \leq 0.7$ [3]. While this *St* window is well documented, a clear demonstration that simply moving *Mc* through a critical value extinguishes the loop under otherwise comparable conditions has not yet been published [3].

Many numerical studies have been attempted, but boundary reflections and scattered parameter sweeps have made it hard to identify which variable governs tone production. The present work uses high-order WENO-5 simulations to tackle three practical questions: predicting onset, estimating peak load, and defining safe operating windows [4]. First, a reference pulsating case is simulated to establish the feedback loop. Then, with all other inputs fixed, (NPR, h (30 - 50 mm), and *Mc*

(0.82 - 1.20) are varied one at a time. A centrally located pressure probe provides clean spectra, and dominant frequencies are converted to Strouhal form to confirm whether they remain within the canonical band whenever the loop survives [5].

2. Numerical Methodology

Numerical simulations are performed using in-house DNS-solver KICK [6].The three-dimensional compressible Navier-Stokes equations for an ideal gas were solved with viscosity and thermal conductivity obtained from Sutherland's law. Inviscid fluxes were calculated using a fifth-order WENO finite-difference scheme with Lax-Friedrichs flux-vector splitting. Viscous fluxes were calculated using central-difference sixth-order scheme, while time integration employed an explicit third-order TVD Runge–Kutta scheme. This high-order, shock-capturing combination supplies the accuracy and stability needed to resolve the jet–plate interaction and its unsteady feedback [7].

2.1. Parametric Study

The computational domain is a 40 mm-long, 50 mm-radius cylindrical ring covering the full 360° azimuth. At initial t=0 a cylindrical jet core (radius 3 mm) is imposed with p_e=1.94 bar, T_e=170 K, axial velocity u_e=496 ms^{-1}; the surrounding ambient is quiescent air at p_∞=1.00 bar, T_∞=293 K. The simulation campaign varied three parameters independently: NPR (by adjusting the static exit pressure while keeping ambient conditions the same), Mc (jet exit velocity set so Mc ranged from 0.82 up to about 1.20), and h (30, 40, or 50 mm measured from nozzle lip to plate; see Table 1). Each case had a run time of 10 ms with uniform $\Delta t = 1.0 \times 10^{-7}$ s.

Table 1: Simulation matrix – input conditions varied (NPR, Mc, plate gap).

Run ID	Expansion	NPR	Mc	h (mm)	Purpose
R1	Under	1.94	0.82	40	Baseline reference (pulsating case)
R2	Over	0.76	1.12	40	Baseline reference (stable case)
R3	Perfect	1	0.82	40	Isolate effect of exit pressure (perfectly expanded)
R4	Over	0.76	0.82	40	Exit pressure variation (over-expanded)
R5	Under	1.94	0.9	40	Mc variation
R6	Under	1.94	0.95	40	Mc variation
R7	Under	1.94	1	40	Mc variation (transition vicinity)
R8	Under	1.94	1.05	40	Mc variation
R9	Under	1.94	1.12	40	Mc variation
R10	Under	1.94	1.2	40	Mc variation
R11	Under	1.94	0.82	50	Plate gap variation (long gap)

2.2. Post-Processing

A single pressure probe located on the centreline, a few millimetres above the nozzle exit and upstream of plate effects records p(t). FFT analysis was used to extract the dominant pulsation frequency. From the frequency, the plate gap, and the jet exit speed, the Strouhal number is computed. RMS pressure fluctuation levels and a three-state classification (pulsating/transition/suppressed) are determined solely from this spectrum. Instantaneous density gradients in all three coordinate directions are also calculated to produce numerical schlieren images that qualitatively confirm the presence or absence of the feedback loop.

3. Results and Discussion

The results are organized from reference behaviour to parametric variation. First, a pulsating reference case establishes the resolved shock–acoustic loop and its spectral signature; a stable reference case then confirms the methodology produces a quiescent state under altered inflow. Subsequent sections isolate the influence of NPR, Mc, and h on loop presence, strength, and frequency.

3.1. Pulsating Jet Reference Configuration

A baseline impinging jet configuration (R1) first simulated. Six density-gradient snapshots (see Fig. 1) illustrate nearly one full pulsation cycle: two successive acoustic waves, generated when the jet core strikes the plate, it propagates upstream toward the nozzle lip, perturb the exit shear layer, and seed the next downstream convective wave packet whose impingement launches the following wave.

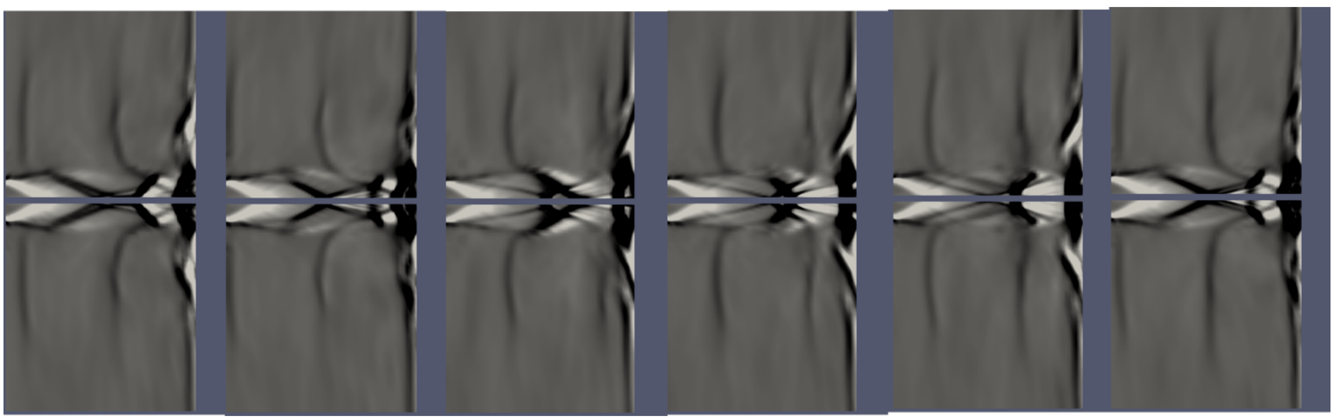

Figure 1: Density-gradient snapshots (baseline, Mc=0.82) showing one feedback cycle; successive plate-generated acoustic waves propagate upstream to the nozzle lip.

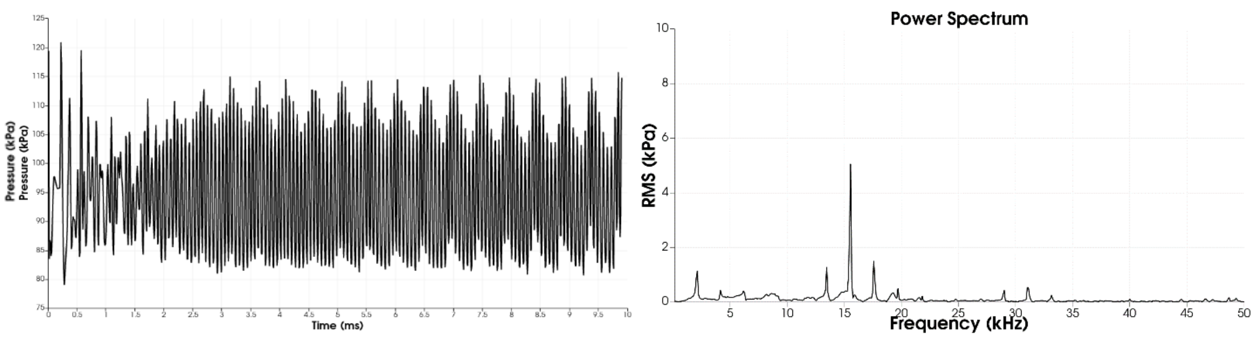

Figure 2: Baseline probe pressure history (post-transient limit cycle) and spectrum with dominant ≈15 kHz tone (St≈0.32)

Figure 2 presents the pressure time history recorded by a center-line probe just above the nozzle. After a brief start-up transient, the signal settles into a train of nearly identical peaks, demonstrating a self-sustained limit cycle. The corresponding Fourier spectrum features a single, narrowband dominant peak with minimal sideband energy. From this peak, we obtain a Strouhal number of approximately 0.32, which is above the 0.3 threshold reported in the literature which validates that the simulation reproduces the key large-scale feedback dynamics observed in physical experiments.

3.2. Stable Jet Reference Configuration

The reference steady case (R2) produces no self-sustained feedback loop. Three density-gradient snapshots (Fig. 3) show only weak, localized adjustments in shear and shock structure, with no coherent upstream acoustic waves. After an initial ≲1.5 ms start-up transient, the probe pressure record (Fig. 4) settles into small, nearly sinusoidal fluctuations without sharp spikes. Its spectrum exhibits only low-level broadband energy and minor low-frequency broadband noise; no distinct peak in the 0.3–0.7 Strouhal band. Because no sharp tonal frequency arises, the computed Strouhal number falls to about 0.03, far below the coherent-pulsation window. Reproducing both this stable regime and periodic feedback loop confirms that the simulation faithfully captures whether the feedback loop is active or inactive. This gives confidence that the subsequent single-parameter sweeps will correctly reveal which physical variable truly governs the onset of acoustic pulsations.

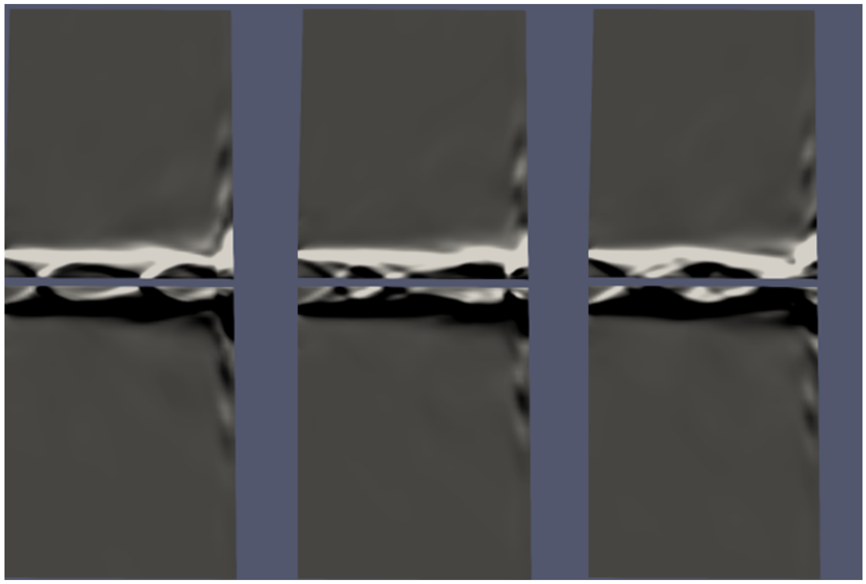

Figure 3: Stable reference case snapshots – absence of upstream acoustic waves (no feedback loop).

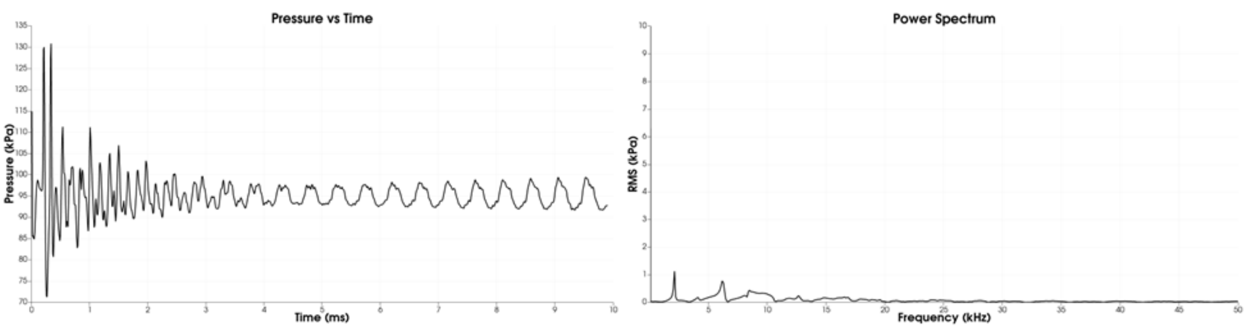

Figure 4: Stable case probe signal and spectrum – low, nearly sinusoidal fluctuations; no narrow peak (St≈0.08).

3.3. Exit Pressure Effects

To assess the effect of NPR on acoustic feedback, the exit static pressure (p_e) was systematically varied while holding all other parameters constant. Starting from the under-expanded reference case (R1), two additional cases were simulated: a perfectly expanded case (R3, Fig.5) and an over-expanded configuration (R4, Fig.6). This controlled variation isolates whether changes in NPR alone are sufficient to suppress or modify the feedback loop. In both modified cases, the probe pressure after a short transient settles into the same sequence of evenly spaced, high-amplitude peaks, and each spectrum shows essentially the same dominant ≈15 kHz tone with similar weak harmonics. The Strouhal values stay in the 0.3–0.7 band, so shifting the NPR by itself neither suppresses the loop nor shifts its frequency. Schlieren pictures confirm that plate-generated acoustic travel upstream and repeat at almost identical cadence for all NPR, indicating that another parameter; not NPR; controls the presence and frequency of the pulsations.

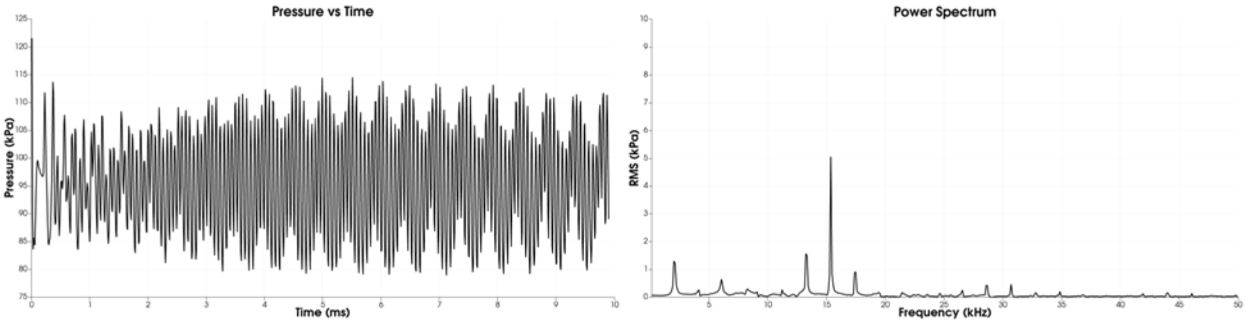

Figure 5: Perfectly expanded jet ($p_e/p\infty \approx 1.0$, Mc=0.82) – limit cycle with ≈15 kHz tone (St≈0.32).

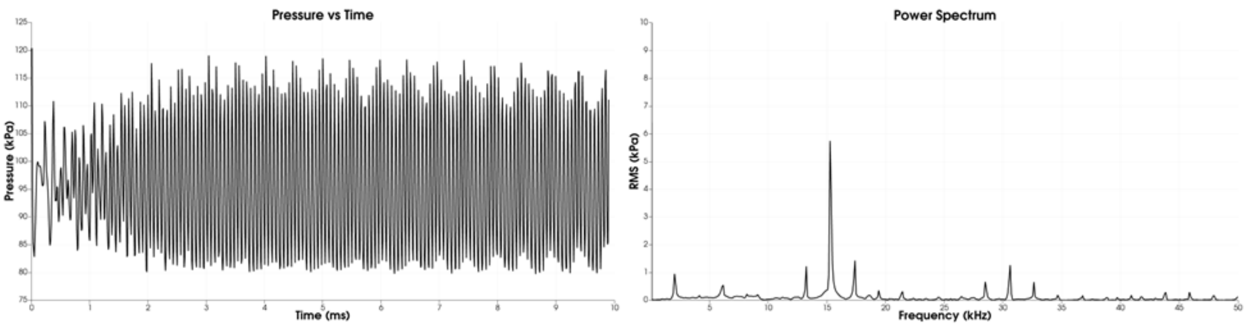

Figure 6: Over-expanded jet ($p_e/p\infty \approx 0.76$, Mc=0.82) – sustained periodic oscillations; ≈15.5 kHz tone (St≈0.32).

3.4. Convective Mach Number Effects

Figure 7 documents the response at Mc = 0.90 (R5). After a brief start-up transient, the pressure trace locks into a train of high, evenly spaced peaks, and the spectrum collapses into a single narrow tone. Identical behaviour appears in the companion sub-unity runs (Mc = 0.82, 0.95; data in Table 2). In this range, an upstream-travelling acoustic wave outruns the downstream-moving vortex packet: it reaches the nozzle lip well before the next roll-up forms, delivers a precisely phased "kick," and so sustains a strong, self-locking cycle. Because compressibility damping is weak below unity, vortices grow large, strike the plate forcefully, and launch the next intense wave. Every case with Mc<1 retains a Strouhal number above 0.30, within the long-established tonal band (0.3 – 0.7) for impinging jets.

When the Mc is increased to unity (R7) as shown in Fig. 8, the organised loop collapses. The pressure record flattens into low, irregular oscillations, and the discrete spectral peak vanishes; the corresponding Strouhal value falls below 0.30. Physically, the acoustic wave and the vortex packet now traverse the gap in almost the same time, so the wave no longer arrives early enough to reinforce shear-layer roll-up. Phase alignment is lost, and the loop cannot re-close, converting what was a sharp tone into weak broadband noise.

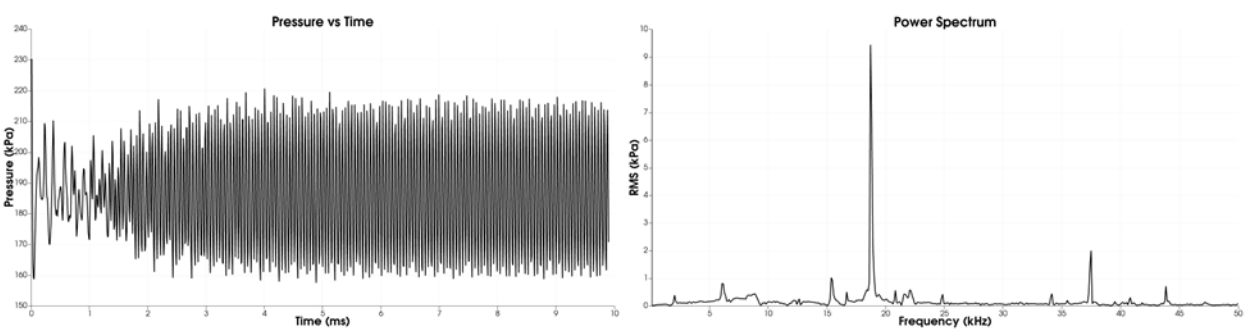

Figure 7: Mc=0.90 – stronger periodic oscillations; single sharp spectral peak (St≈0.33).

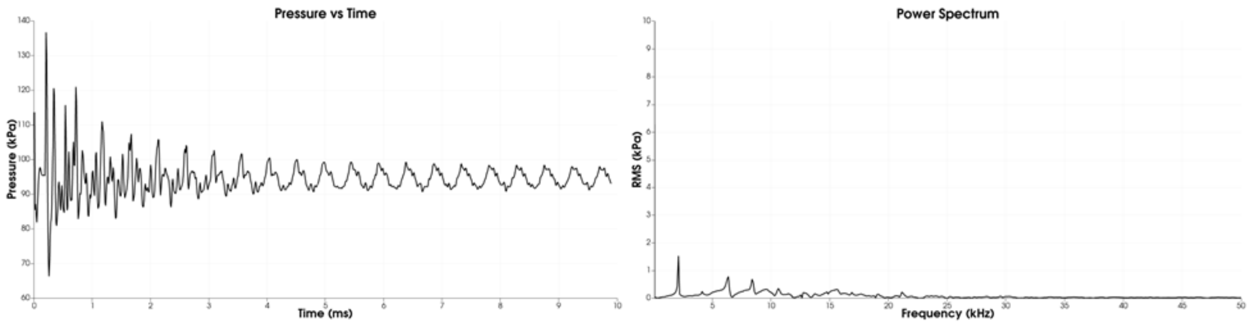

Figure 8: Mc=1.00 – pulsation collapses; only low, irregular fluctuations (St≈0.05).

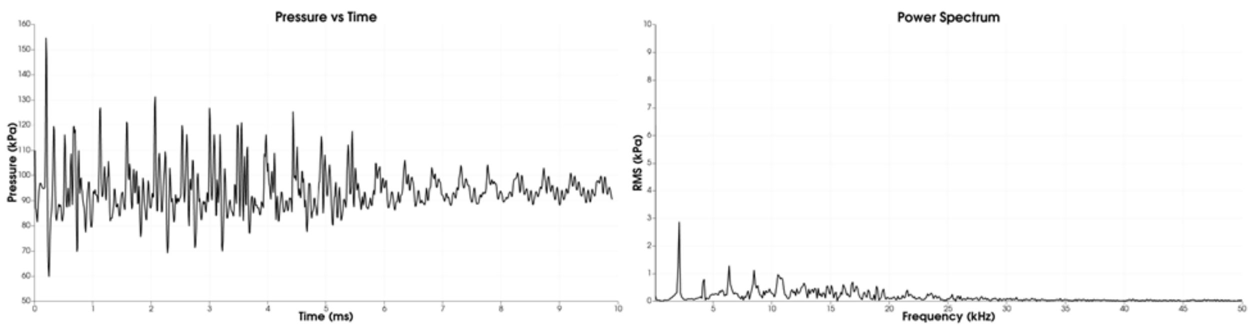

Figure 9: Mc=1.12 – no coherent tone; low-level broadband spectrum (St<0.04).

Further increases in exit velocity reinforce this suppression. Figure 9 shows the Mc = 1.12 result (R9). Spectra are fully broadband, and Strouhal numbers remain below the tonal window. Here, the vortex packet convects downstream faster relative to the nozzle than any acoustic wave can return upstream. By the time a wave reaches the lip, the shear-layer segment that might have been energised has already departed. Concurrently, higher compressibility damps Kelvin–Helmholtz growth, so plate impacts generate only diffuse, low-energy pressure bursts. Loop gain, therefore, stays below the threshold for self-sustained oscillation: just above unity, the signal is almost silent, while at higher Mc the broadband level rises with jet kinetic energy, but no discrete tone re-emerges. Similar effects can be notices in other cases (R6 & R10) with Mc>1.

Table 2: Output metrics – peak frequency and Strouhal number for all simulated cases.

Case	Mc	Peak f (kHz)	Strouhal No
R1	0.82	15.5	0.32
R2	1.12	2	0.03
R3	0.82	15	0.32
R4	0.82	15.5	0.32
R5	0.9	18	0.33
R6	0.95	19.8	0.345
R7	1	2.5	0.05
R8	1.05	2.4	0.04
R9	1.12	2	0.03
R10	1.2	2	0.02
R11	0.82	17	0.34

3.5. Plate Gap Effects

Figure 10 presents the h = 30 mm case (R10). Decreasing the plate gap strengthens the feedback loop: the probe pressure quickly settles into very regular, high-amplitude peaks, and the power spectrum displays a single sharp tone at ≈ 19.5 kHz (St ≈ 0.38). Figure 11 presents the h = 50 mm case (R11). Increasing the gap slightly lowers loop gain and shifts the tone down to ≈ 17 kHz (St ≈ 0.34) with mild amplitude modulation, yet the spectral peak remains narrow and dominant. In both scenarios, the Strouhal number remains within the 0.30–0.70 band, confirming that plate spacing fine-tunes amplitude and frequency but does not extinguish the acoustic feedback loop.

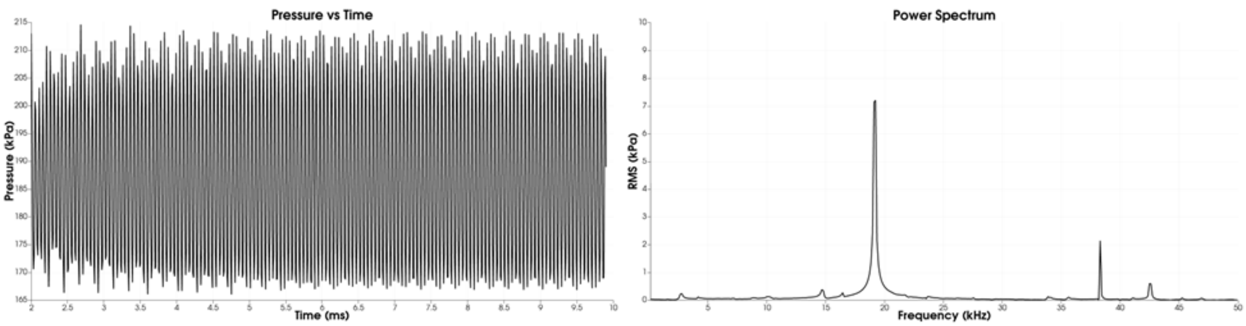

Figure 10: h=30 mm (Mc=0.82) – strong steady pulsation; ≈19.5 kHz tone (St≈0.38).

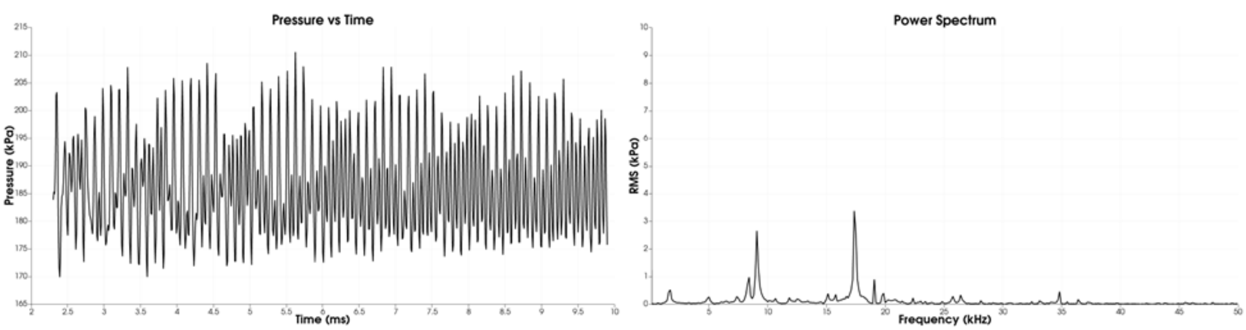

Figure 11: h=50 mm (Mc=0.82) – weaker, slightly modulated pulsation; ≈17 kHz tone (St≈0.34).

4. Conclusion

This finding offers a valuable design parameter for supersonic nozzle configurations in aerospace applications. High-order numerical simulations of an impinging jet were used to identify which factor governs coherent flow pulsations. Three parameters were varied independently: NPR, h and Mc, and only Mc acted as a true switch. Altering NPR or h changed loop strength and frequency but never quenched the tone. By contrast, sub-sonic Mc (0.82–0.95) yielded a single stable tone, Mc ≈ 1 abruptly collapsed the oscillation, and Mc > 1 resulted in only broadband fluctuations. Thus, for this geometry, Mc ≈ 1 delineates organized feedback loop, offering a simple guideline: design for Mc ≥ 1 to suppress discrete tonal loading, or Mc < 1 when strong pulsation is desired.

References

[1] A. Krothapalli, E. Rajkuperan, F. Alvi, and L. Lourenco, "Flow field and noise characteristics of a supersonic impinging jet," *J. Fluid Mech.*, vol. 392, pp. 155–181, Aug. 1999, doi: 10.1017/S0022112099005406.

[2] D. M. Mitchell, D. R. Honnery, and J. Soria, "The visualization of the acoustic feedback loop in impinging underexpanded supersonic jet flows using ultra-high frame rate schlieren," *J. Vis.*, vol. 15, no. 4, pp. 333–341, Nov. 2012, doi: 10.1007/s12650-012-0139-9.

[3] B. Henderson, J. Bridges, and M. Wernet, “An experimental study of the oscillatory flow structure of tone-producing supersonic impinging jets,” *J. Fluid Mech.*, vol. 542, pp. 115–137, Nov. 2005, doi: 10.1017/S0022112005006385.
[4] G.-S. Jiang and C.-W. Shu, “Efficient Implementation of Weighted ENO Schemes,” *J. Comput. Phys.*, vol. 126, no. 1, pp. 202–228, June 1996, doi: 10.1006/jcph.1996.0130.
[5] D. Papamoschou and A. Roshko, “The compressible turbulent shear layer: an experimental study,” *J. Fluid Mech.*, vol. 197, pp. 453–477, Dec. 1988, doi: 10.1017/S0022112088003325.
[6] I. Klioutchnikov, H. Olivier, and J. Odenthal, “Numerical investigation of coaxial jets entering into a hot environment,” *Comput. Fluids*, vol. 86, pp. 490–499, Nov. 2013, doi: 10.1016/j.compfluid.2013.07.032.
[7] T. J. Poinsot and S. K. Lele, “Boundary conditions for direct simulations of compressible viscous flows,” *J. Comput. Phys.*, vol. 101, no. 1, pp. 104–129, July 1992, doi: 10.1016/0021-9991(92)90046-2.